SERBIAN JOURNAL OF ELECTRICAL ENGINEERING
Vol. 15, No. 1, February 2018, 41-52

UDC: 666.655:531.8]:004.42MATLAB **DOI: https://doi.org/10.2298/SJEE1801041J**

A Matlab/Simulink 3D Model of Unsymmetrical Ultrasonic Sandwich Transducers

Igor Jovanović[1], Uglješa Jovanović[1], Dragan Mančić[1]

Abstract: Ultrasonic sandwich transducer is a half-wave resonant structure which oscillates in thickness direction. This paper presents a new Matlab/ Simulink model of a prestressed unsymmetrical ultrasonic sandwich transducer, which is modeled by applying three-dimensional (3D) Matlab/Simulink models of piezoceramic rings and metal endings derived from the piezoceramic ring model. With the cascade connection of the piezoceramic rings model with metal endings model, a complete model of ultrasonic transducer is obtained. Using this model one may determine any transducer transfer function, whereat is taken into the account the external medium influence, as well as the influence of the thickness and radial modes of each transducer component. The electro-mechanical equivalent circuit of the hammer transducer, which represents one-dimensional (1D) model, is also derived and presented in this paper. The comparisons between experimental and theoretical results are quite good and validate the new analytical 3D design approach.

Keywords: Matlab/Simulink Model, Analytical 3D Model, Electrical Impedance Characteristics, Ultrasonic Sandwich Transducer.

1 Introduction

Implementation of ultrasonic transducers began in 1917, when Paul Langevin designed the first piezoelectric sandwich transducer [1]. In nowadays, application of power ultrasound is implemented in many branches of industry such as mining, ultrasonic machining, material processing, cutting, welding [2 – 4], sonochemistry [5, 6] and other ultrasonic liquid processing applications [7].

Ultrasonic sandwich transducer, also known a Langevin's transducer, is a half-wave resonant structure which employs a high frequency high voltage to generate mechanical vibrations, with the help of piezoelectric effect. Most importantly, by using its natural longitudinal vibration in combination with adjustment of geometrical dimensions, a transducer can resonate at the desired frequency. Thanks to the advantages of high electromechanical coupling factor, piezoelectric constant and fast response, piezoceramics are widely used in many fields, including the ultrasonic applications. Ultrasonic sandwich transducer

[1]University of Niš, Faculty of Electronic Engineering, 14 Aleksandra Medvedeva, 18000 Niš, Serbia;
E-mails: igor.jovanovic@elfak.ni.ac.rs, ugljesa.jovanovic@elfak.ni.ac.rs and dragan.mancic@elfak.ni.ac.rs

generally consists of a piezoceramic stack (Blocks 1 and 2, shown in Fig. 1), a front mass which is most often also called a emitter (Blocks 3 and 4, shown in Fig. 1), which can double as a waveguide that fix the resonance frequencies of the system, a back mass which is most often also called a reflector (Blocks 5, 6 and 7, shown in Fig. 1), and a central bolt (Blocks 8, 9, 10 and 11, shown in Fig. 1). Transducer in which the plane of the oscillating node divides the ceramic equally is referred to as a symmetric transducer in which metal endings may be made out of same or different materials. If in fact the middle of the ceramic is not in the oscillating node, transducer is referred to as an unsymmetrical transducer. It is common to refer to a transducer with metal endings made of different material as an unsymmetrical transducer, regardless if the neutral plane is located in the middle of the piezoceramic.

Enhancement of ultrasonic transducer performances requires a detailed investigation of the mechanical and electrical properties for different operating conditions. Modeling of more complete transducer constructions is not possible using 1D model, which is based on calculations from electromechanical equivalent circuit as a result based on the similarity between mechanical vibration and electrical resonance. 1D vibration theory is used where the longitudinal transducer dimension is greater than the lateral dimension, therefore only the thickness modes are considered and vibrations in other directions are neglected [8].

The research presented in this paper analyses the Matlab/Simulink 3D matrix model of the prestressed unsymmetrical ultrasonic sandwich transducer. Ultrasonic sandwich transducer is modelled using the approximate 3D matrix model previously proposed in paper [9], which takes into the account thickness and radial modes of oscillation as well as their mutual coupling. Due to the complexity of the transducer structure and implementation of the 3D model, following modular solutions are developed first: The model of a piezoceramic ring is presented in [10] as networks with four mechanical and the single electrical contacts; The model of passive metal endings is presented in [11], where metal parts are represented as networks with four or three contacts. These analytical models can be easily implemented in a simple program and they are useful for design of a piezoelectric vibrating system even when fast calculations are required.

2 A Matlab/Simulink 3D Matrix Model of the Ultrasonic Transducer

The proposed model of the ultrasonic sandwich transducer is consisted of a single pair of piezoceramic rings which are connected mechanically in series and electrically in parallel. One could obtain a 3D electromechanical model of the ultrasonic sandwich transducer (see Fig. 1) if all transducer components are connected in series and in parallel [12]. By applying an AC exiting voltage on transducer electrical contacts and a proper ambient acoustic impedances on the mechanical contacts it is possible to obtain each transducer transfer function.

It should be noted that each model block consists two components. Namely, the first one is responsible for calculation of all elements of the matrix model based on the inserted material properties. The second component solves equation systems by using the results from the first component.

Models of piezoceramic rings have two blocks. Their role is to initialize values of forces F_3 and F_4 acting from direction of the second piezoceramic and reflector, which are obtained from Block 2 and Block 5 respectively. Based on the inserted ceramic properties, all elements are calculated $A_{i,j} = z_{i,j}$ (i, j = 1, 2, 3, 4, 5) [9], including all necessary elements of the equation system (1):

$$\begin{bmatrix} 0 \\ 0 \\ E_3 \\ E_4 \\ E_5 \end{bmatrix} = \begin{bmatrix} A_{11} & A_{12} & A_{13} & A_{14} & A_{15} \\ 0 & a_{11} & a_{12} & a_{13} & a_{14} \\ 0 & 0 & b_{11} & b_{12} & b_{13} \\ 0 & 0 & 0 & c_{11} & c_{12} \\ 0 & 0 & 0 & c_{21} & c_{22} \end{bmatrix} \begin{bmatrix} \nu_1 \\ \nu_2 \\ \nu_3 \\ \nu_4 \\ I \end{bmatrix}, \tag{1}$$

where:

$$\begin{aligned} a_{i,j} &= A_{1,j+1}A_{i+1,1} - A_{1,1}A_{i+1,j+1}, \quad (i, j = 1,2,3,4), \\ b_{i,j} &= a_{1,j+1}a_{i+1,1} - a_{1,1}a_{i+1,j+1}, \quad (i, j = 1,2,3), \\ c_{i,j} &= b_{1,j+1} \cdot b_{i+1,1} - b_{1,1} \cdot b_{i+1,j+1}, \quad (i, j = 1,2), \end{aligned} \tag{2}$$

and:

$$\begin{aligned} E_3 &= A_{11}a_{11}F_1, \\ E_4 &= A_{11}a_{11}b_{12}F_3 - A_{11}a_{11}b_{11}F_4, \\ E_5 &= A_{11}a_{11}b_{31}F_3 - A_{11}a_{11}b_{11}U. \end{aligned} \tag{3}$$

It should be noted that two models of piezoceramic rings, i.e. Block 1 and Block 2 (equation system (4)), do not have the same matrix of equation system, which consequently makes their solutions to be different. This difference originates from the existence of contact ring-shaped surfaces between ceramics, i.e. mechanical velocities on these surfaces, which are calculated in Block 1. Mechanical forces acting on the joint surfaces are the same. However, although mechanical velocities have the same intensity their directions are opposite.

$$\begin{bmatrix} 0 \\ 0 \\ E_3 \\ E_5 \end{bmatrix} = \begin{bmatrix} A_{11} & A_{12} & A_{13} & A_{14} & A_{15} \\ 0 & a_{11} & a_{12} & a_{13} & a_{14} \\ 0 & 0 & b_{11} & b_{12} & b_{13} \\ 0 & 0 & 0 & c_{21} & c_{22} \end{bmatrix} \begin{bmatrix} \nu_1 \\ \nu_2 \\ \nu_3 \\ \nu_4 \\ I \end{bmatrix}. \tag{4}$$

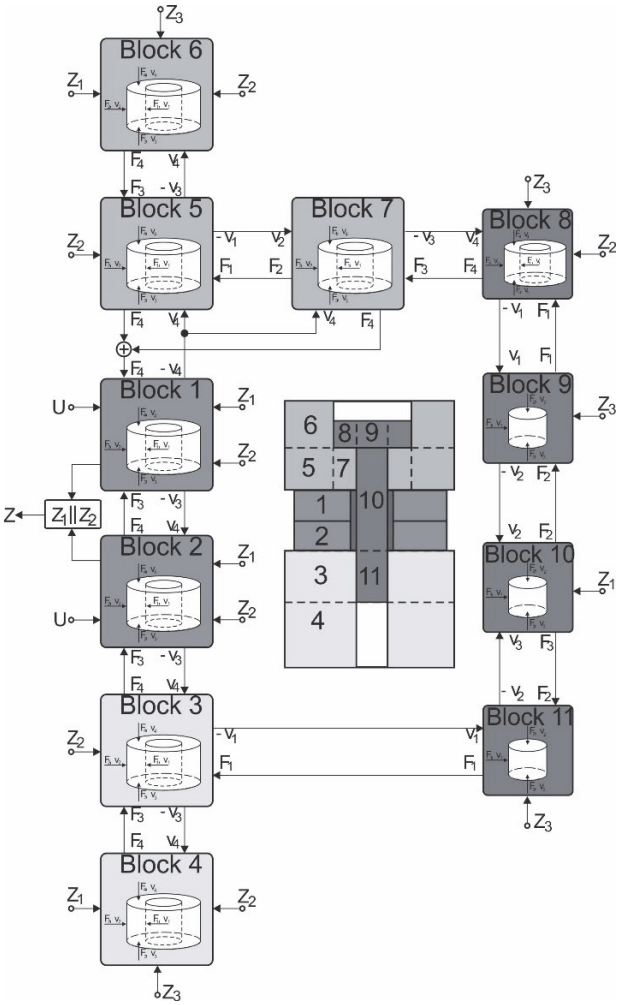

Fig. 1 – *Block diagram of the ultrasonic transducer model.*

Along with the electrical impedance *Z*, which is from standpoint of the power supply connected in parallel with the electrical impedance of Block 1 (piezoelectric element), outputs of Block 2 are mechanical force and velocity, which act on the ring-shaped surfaces towards the Block 1 ($F_4 = A_{13}v_1+A_{23}v_2+A_{34}v_3+A_{44}v_4+A_{35}I$) and towards the transducer emitter ($-v_3$).

Models of the emitter and reflector comprise two parts which are described in Block 3 and Block 4, for the emitter, and in Block 5 and Block 6, for the reflector. By analyzing geometrics of these two parts and their connection with the remaining transducer components, the similarity between models of Block 4 and Block 6 can be observed. The same can be concluded for Block 3 and Block

5, with only discrepancy being material properties and their geometrics. Equation systems, which in the frequency domain characterizes Block 3, is given in expression (5) and in case of Block 4 in (6):

$$\begin{bmatrix} F_1 \\ F_1 A_{12} \\ H_3 \end{bmatrix} = \begin{bmatrix} A_{11} & A_{12} & A_{13} & A_{14} \\ 0 & a_{11} & a_{12} & a_{13} \\ 0 & 0 & b_{11} & b_{12} \end{bmatrix} \begin{bmatrix} \nu_1 \\ \nu_2 \\ \nu_3 \\ \nu_4 \end{bmatrix}, \tag{5}$$

$$\begin{bmatrix} 0 \\ 0 \\ 0 \end{bmatrix} = \begin{bmatrix} A_{11} & A_{12} & A_{13} & A_{14} \\ 0 & a_{11} & a_{12} & a_{13} \\ 0 & 0 & b_{11} & b_{12} \end{bmatrix} \begin{bmatrix} \nu_1 \\ \nu_2 \\ \nu_3 \\ \nu_4 \end{bmatrix}, \tag{6}$$

wherein $H_3 = A_{11}a_{11}F_3 + \left(A_{21}a_{21} - A_{31}a_{11}\right)F_1$.

Mechanical velocities (v_1, v_2 and v_3) and velocity on the ring-shaped surface towards the piezoceramic (v_4), obtained from Block 2, are used to calculate the mechanical force F_4 acting towards the piezoceramic.

The obtained mechanical velocity on the ring-shaped surface towards the second part of the emitter v_3 is forwarded to Block 4 in which in combination with the acoustic input impedances used to calculate force F_4 acting on that surface.

The central bolt is represented by Blocks 8, 9, 10 and 11. Based on the physical connections, which certain central bolt parts have with the remaining transducer components, an analogy between Block 9 and Block 11 can be observed. Consequently, only Block 9 will be presented in the paper and its outputs are mechanical velocities, which act on the cylindrical surfaces towards the middle part of the central bolt, i.e. towards Block 10, and mechanical forces acting on the cylindrical surfaces of the central bolt towards the appropriate parts of the reflector/emitter. Equation system, which in the frequency domain characterizes Block 9 is given in (7):

$$\begin{bmatrix} F_2 \\ 0 \end{bmatrix} = \begin{bmatrix} A_{21} & A_{22} & A_{23} \\ A_{31} & A_{32} & A_{33} \end{bmatrix} \begin{bmatrix} v_1 \\ v_2 \\ v_3 \end{bmatrix}. \tag{7}$$

Model of the middle part of the central bolt has the simplest structure. Based on this model, in each simulation step the following instructions are performed: initialization of mechanical forces acting on the joint surfaces of all transducer components; calculation of mechanical velocities on the same surfaces using known values of ambient acoustic impedances acting on the

appropriate transducer components; acquisition of final and accurate initial mechanical forces. All aforementioned is performed using the circuit for solving equations (8):

$$\begin{aligned} \nu_1 &= \frac{A_{12}\nu_2 + A_{13}\nu_3}{-A_{11}}, \\ F_2 &= A_{21}\nu_1 + A_{22}\nu_2 + A_{23}\nu_3, \\ F_3 &= A_{31}\nu_1 + A_{32}\nu_2 + A_{33}\nu_3. \end{aligned} \tag{8}$$

By observing Fig. 1 it can be concluded that the ring-shaped reflector parts (Block 5 and Block 7) are in mechanical series connection with the piezoelectric element (Block 1). This connection in the transducer model is represented with the adder circuit of the reflector mechanical forces in the direction of the piezoelectric element, while value of mechanical velocity on the ring-shaped surface of the piezoelectric element is directly forwarded to the mentioned parts of the reflector.

Block 7 is used to solve equation system (9) in which are known mechanical velocities v_2 and v_4, and mechanical force F_3.

$$\begin{bmatrix} 0 \\ F_3 \end{bmatrix} = \begin{bmatrix} A_{11} & A_{12} & A_{13} & A_{14} \\ A_{31} & A_{32} & A_{33} & A_{34} \end{bmatrix} \begin{bmatrix} \nu_1 \\ \nu_2 \\ \nu_3 \\ \nu_4 \end{bmatrix}. \tag{9}$$

Upon calculating values of v_2 and v_4, the remaining mechanical forces are calculated as $F_2 = A_{21}v_1+A_{22}v_2+A_{23}v_3+A_{24}v_4$ and $F_4 = A_{41}v_1+A_{42}v_2+A_{43}v_3+A_{44}v_4$.

Ring-shaped part of the central bolt head located above the reflector is, in contrast to the rest of the central bolt, represented by the four-port network (Block 8) because of its physical dimensions (ring structure). In this block, equation system (5) is solved, but in this case it applies $H_3 = A_{21}a_{21}F_1–A_{31}a_{11}F_1$.

2.1 Resonance frequency equations of the unsymmetrical transducer

To demonstrate capabilities of the proposed 3D model, a 1D model is derived. In order to calculate the input electrical impedance of the unsymmetrical transducer based on similarity between mechanical vibration and electrical resonance of the electromechanical equivalent circuit shown in Fig. 2, electromechanical equivalent 1D method is adopted. Elements of this circuit, which correspond to piezoceramic rings and isotropic, asymmetric metal endings, made out of different materials with different lengths, are determined based on the following expressions:

$$Z_{p1} = \mathrm{j}Z_{cp}\tan\frac{nk_p l_p}{2}, \quad Z_{p2} = \frac{-\mathrm{j}Z_{cp}}{\sin(nk_p l_p)}, \tag{10}$$

$$Z_{i1} = \mathrm{j} Z_{ci} \tan\frac{k_i l_i}{2}, \quad Z_{i2} = \frac{-\mathrm{j} Z_{ci}}{\sin(k_i l_i)}, \tag{11}$$

where $Z_{cp} = \rho_p v_p P_p$ and $k_p = \omega/v_p$; Z_{cp} is characteristic impedance of the piezoceramic; ρ_p is density, l_p and P_p are lengths and areas of the piezoceramic; v_p is velocity of the longitudinal ultrasonic waves through the piezoceramic; n is number of the piezoceramics; $C_0 = n\varepsilon_{33}^S S_p / l_p$ is cut-off capacitance; $N = h_{33}C_0/n$ is electromechanical conversion coefficient of the piezoceramic; V is voltage applied on the transducer; $Z_{ci} = \rho_i v_i P_i$ and $k_i = \omega/v_i$ (for i = 1, 2 and 3), Z_{ci} are characteristic impedances of the metal elements; ρ_i is density, l_i and P_i are lengths and areas of the metal elements; v_i are velocities of longitudinal ultrasonic waves through the metal elements; Z_{bl} and Z_{fl} are radiant impedances of the transducer in the back and front directions.

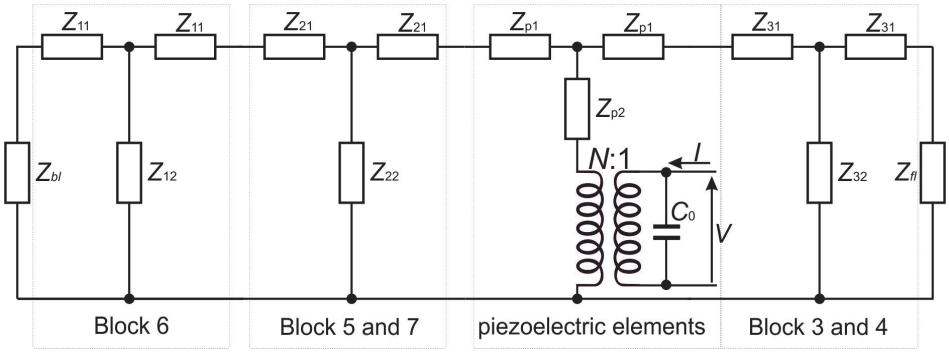

Fig. 2 – *Electromechanical equivalent circuit of the unsymmetrical ultrasonic transducer.*

Based on Fig. 2, the input electric impedance of the transducer can be obtained as:

$$Z_e = \frac{N^2 Z_e}{1 + j\omega C_0 N^2 Z_m}, \tag{12}$$

where $\omega = 2\pi f$ and expressions for Z_m is:

$$Z_m = Z_{p2} + \frac{Z_{ef} Z_{eb}}{Z_{ef} + Z_{eb}}, \tag{13}$$

where

$$Z_{ef} = Z_{31} + Z_{p1} + \frac{(Z_{fl} + Z_{31})Z_{32}}{Z_{fl} + Z_{31} + Z_{32}}, \tag{14}$$

$$Z_{eb} = Z_{21} + Z_{p1} + \frac{\left(Z_{11} + \frac{(Z_{bl} + Z_{11})Z_{12}}{Z_{bl} + Z_{11} + Z_{12}} + Z_{21} \right) Z_{22}}{Z_{11} + \frac{(Z_{bl} + Z_{11})Z_{12}}{Z_{bl} + Z_{11} + Z_{12}} + Z_{21} + Z_{22}}. \quad (15)$$

3 Results and Discussion

The calculated and experimental results are obtained using a PZT8 piezoceramic equivalent material [13] with dimensions Ø38/Ø15/5mm. The reflector and central bolt are made out of stainless steel with parameters: density 7800 kg/m^3, Poisson's ratio 0.29 and Young's modulus of elasticity $2.09 \cdot 10^{11}$ N/m^2. The emitter is made out of duralumin with parameters: density 2790 kg/m^3, Poisson's ratio 0.34 and Young's modulus of elasticity $0.68 \cdot 10^{11}$ N/m^2. It should be noted that the electrical impedance measurements are performed using HP4194A Impedance/Gain-Phase Analyzer.

The input electrical impedance of the ultrasonic transducer and mechanical impedances on the particular transducer outer surfaces are obtained from the 3D model. All blocks are masked (*mask-block*) and their parameters are inserted in the window that opens on double clicking the corresponding block. For piezoceramic rings, part of this window is shown in Fig. 3a, while the entire window in case of metal extensions is shown in Fig. 3b.

Fig. 3a shows inserted parameters for the ceramic used in the laboratory. To insert parameters for a non-predefined ceramic it necessary to select the "User-defined" option in the popup menu, this enables insertion of all ceramic parameters individually.

If the designation of transducer components adopts the notation shown in Fig. 1, simulated transducers have the dimensions given in **Table 1**.

Table 1

Dimensions of transducers used in experiment.

Dimension (mm)	Transducer1			Transducer2		
	Thickness	Outer diameter	Inner diameter	Thickness	Outer diameter	Inner diameter
Block 3	18.7	40	8	18	39.8	8
Block 4	23.3	40	8	0.2	39.8	8
Block 5	16.3	40	13.15	11.2	40	13.1
Block 6	15.2	40	13.15	0.8	40	13.1
Block 7	16.3	13.15	8	11.2	13.1	8
Block 8	8	13.15	8	8	13.1	8
Block 9	8	8	/	8	8	/
Block 10	26.3	8	/	21.2	8	/
Block 11	18.7	8	/	18	8	/

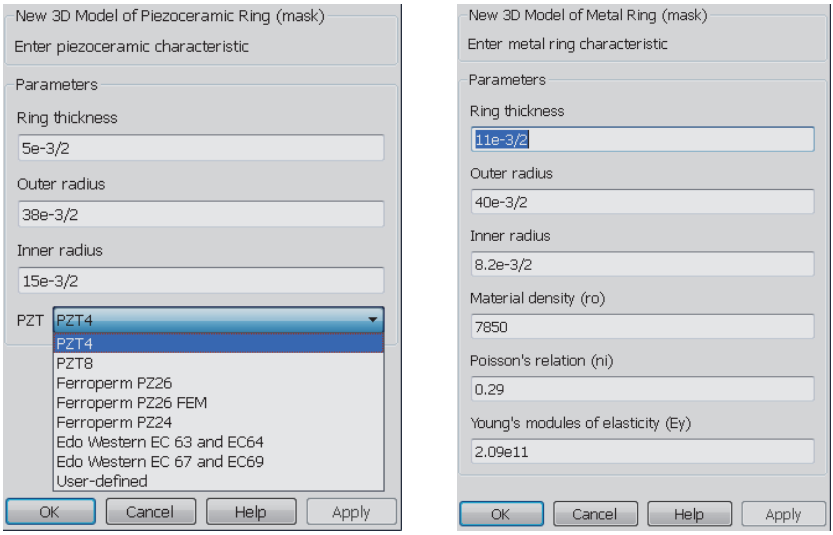

(a) (b)

Fig. 3 – *Interface for insertion of piezoceramic parameters (a) and metal ending parameters (b).*

Figs. 4 and 5 shows the measured frequency characteristic of the ultrasonic transducer under low power level. Based on these measurements it can be seen that the input electrical impedance is in correspondence with the simulated curves.

In order to demonstrate accuracy of the 3D model, Fig. 4 also shows the simulated frequency characteristic of the Transducer1 with the proposed 1D model (12). Fig. 4 clearly shows that the proposed 3D model, which takes into the account coupling of oscillations in both radial and thickness directions, would be ideal. In case of the transducer with short metal endings, frequency errors in the 1D model are more pronounced, that is for Transducer2 with small axial dimensions, this 1D model makes a big errors in predicting resonant modes, so it is advisable to use accesses in transducer modelling using apparent elasticity moduli method [14].

The frequency dependency of the mechanical impedance on a free ring-shaped emitter surface can be obtained with minor adjustments of the transducer model. This is especially important in applications in which transducer is used as a sensor or as an energy harvesting device. In the first case for Transducer2, the mechanical impedance is calculated when electrical contacts are short circuit that is when the output voltage is zero (U = 0 V). The resonant and antiresonant frequencies obtained from the transducer model, when electrical connections are short circuit, are f_{asc}= 19.8 kHz and f_{rsc}= 40 kHz. In the second case, the

mechanical impedance is calculated when electrical contacts are left open that is when the input current is zero ($I = 0$ A). The resonant and antiresonant frequencies obtained from the transducer model, when electrical contacts are left open, are f_{aoc}= 21.1 kHz and f_{roc}= 45.3 kHz.

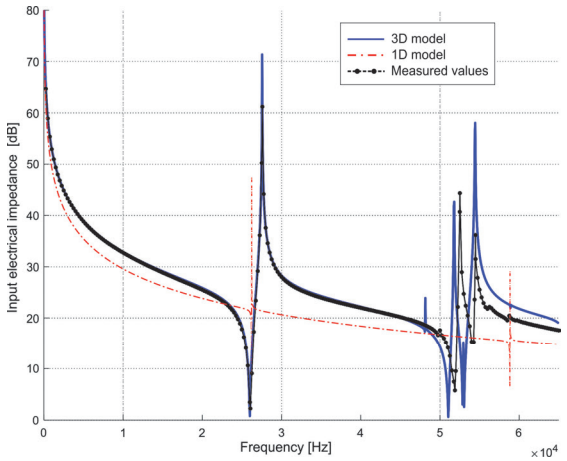

Fig. 4 – *Simulated and experimental input electrical impedance versus frequency for the Transducer1.*

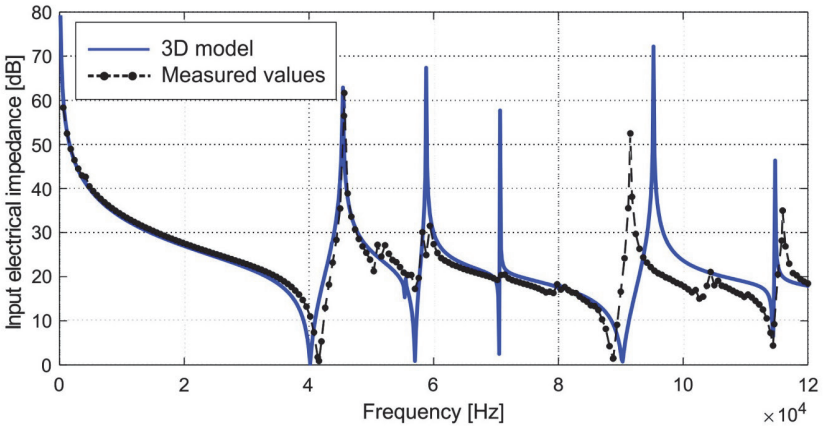

Fig. 5 – *Simulated and experimental input electrical impedance versus frequency for the Transducer2.*

The results of this analysis are easily obtained due to the nature of the model implemented in Matlab/Simulink. The frequency error depends on the standard material parameters of the piezoelectric elements and the metal endings are used in the theoretical calculation. In addition, the mechanical and the dielectric losses in the composite transducer are ignored in calculations. All

above presented results, obtained from model and measurements, are for piezoceramics electrically connected in parallel.

4 Conclusion

The ideal model, which takes into the account all parameters, boundary conditions, all existing resonant modes and conditions on which the transducer properties depend, cannot be possibly realized. Therefore, the presented analysis aims to obtain as comprehensive as possible, but yet simple model, which, although it is approximate, takes into the consideration as much beginning parameters as possible. In the first step, the electromechanical equivalent circuit was derived and the frequency equations were obtained by using the analytic method. The 1D analysis theory requires that the radial dimension is much shorter than the longitudinal dimension. When the axial dimension of the transducer is decreased, the radial vibration becomes intense. In this case, the 3D coupled vibration should be considered.

Based on the presented 3D model, it is possible to synthesize the transducer with predefined properties and given resonant frequency, which was in fact the aim of the presented analysis. Based on the results obtained by applying the proposed transducer models, several transducers that were not presented in this paper were also realized. All of them have been tested in many applications. The measurement results of electrical properties of the obtained electromechanical systems validate this design approach.

5 Acknowledgement

This work was supported by the Ministry of Education, Science and Technological Development of the Republic of Serbia under the project TR33035.

6 References

[1] P. Langevin: French Patent, Nos: 502913 (29.5.1920); 505703 (5.8.1920); 575435 (30.7.1924).

[2] Z. Wang, J. Zeng, H. Song, F. Li: Research on Ultrasonic Excitation for the Removal of Drilling Fluid Plug, Paraffin Deposition Plug, Polymer Plug and Inorganic Scale Plug for Near-well Ultrasonic Processing Technology, Ultrasonics Sonochemistry, Vol. 36, 2017, pp.162 − 167.

[3] J. Li, T. Monaghan, T. T. Nguyen, R. W. Kay, R. J. Friel, R. A. Harris: Multifunctional Metal Matrix Composites with Embedded Printed Electrical Materials Fabricated by Ultrasonic Additive Manufacturing, Composites Part B: Engineering, Vol.113, 2017, pp.342 − 354.

[4] S. Kumar, C. S. Wu, G. K. Padhy, W. Ding: Application of Ultrasonic Vibrations in Welding and Metal Processing: A Status Review, Journal of Manufacturing Processes, Vol.26, 2017, pp. 295 – 322.

[5] N. Pokhrel, P. K. Vabbina, N. Pala: Sonochemistry: Science and Engineering, Ultrasonics Sonochemistry, Vol. 29, 2016, pp. 104 − 128.

[6] K. Gotoh, K. Harayama: Application of Ultrasound to Textiles Washing in Aqueous Solutions, Ultrasonics Sonochemistry, Vol. 20, No. 2, 2013, pp. 747 − 753.

[7] N. N. Mahamuni, Y. G. Adewuyi: Advanced Oxidation Processes (AOPs) Involving Ultrasound for Waste Water Treatment: A Review with Emphasis on Cost Estimation, Ultrasonics Sonochemistry, Vol. 17, No. 6, 2010, pp. 990 − 1003.

[8] S. Lin, H. Tian: Study on the Sandwich Piezoelectric Ceramic Ultrasonic Transducer in Thickness Vibration, Smart Materials and Structures, Vol. 17, No. 1, 2008, pp. 1 − 9.

[9] D. Mančić, G. Stančić: New Three-dimensional Matrix Models of the Ultrasonic Sandwich Transducers, Journal of Sandwich Structures and Materials, Vol. 12, No. 1, 2010, pp. 63 − 80.

[10] I. Jovanović, D. Mančić, V. Paunović, M. Radmanović, Z. Petrušić: A Matlab/Simulink Model of Piezoceramic Ring for Transducer Design, ICEST 2011, Vol. 3, 2011, pp. 952 − 955.

[11] I. Jovanović, D. Mančić, V. Paunović, M. Radmanović, V.V. Mitić: Metal Rings and Discs Matlab/Simulink 3D Model for Ultrasonic Sandwich Transducer Design, Science of Sintering, Vol. 44, No. 3, 2012, pp. 287 − 298.

[12] I. Jovanović, U. Jovanović, D. Mančić: A Matlab/Simulink Model of a Langevin's Ultrasonic Power Transducers, 4th International Conference on Electrical, Electronics and Computing Engineering, IcETRAN 2017, Kladovo, Serbia, June 05-08, 2017, pp. ELI3.5.1 – 5.

[13] Five piezoelectric ceramics, Bulletin 66011/F, Vernitron Ltd., 1976.

[14] E. Mori, K. Itoh, A. Imamura: Analysis of a Short Column Vibrator by Apparent Elasticity Method and its Application, Ultrasonics International, 1977, Conference Proceedings, pp.262 − 266.